FREEZING STOCHASTIC TRAVELLING WAVES

G. J. LORD* AND V. THÜMMLER†

Abstract. We consider in this paper a new method for computing stochastic travelling waves that freezes the wave in the computational domain so it does not move. We obtain a stochastic partial differential algebraic equation that we then discretize and solve. We compare this to a standard approach of simply solving a stochastic partial differential equation directly and examine wave profiles and wave speeds for the Nagumo equation. We examine the effect of multiplicative and additive noise on the speed of propagation with the noise intensity. For multiplicative Itô noise the wave speed is not always strictly increasing with noise intensity. We illustrate that the method can be applied when nucleation of new stochastic travelling waves occurs with additive noise. Finally we compute using a weaker notion of wave speed to freeze the travelling wave.

1. Introduction. The effects of stochastic forcing on solutions of stochastic partial differential equations (SPDEs) has recently received a great deal of attention in applications ranging from material science, atmosphere modelling to neural science. Of particular interest are the effects of noise on travelling waves and fronts as these are often physically important solutions. We use the term travelling wave to include both travelling and pulses, fronts and waves and we develop in this paper numerical methods to solve for stochastic versions of these objects.

We consider the stochastic PDE

$$du = \Big[u_{xx} + f(u)\Big]\, dt + g(u,t)dW(t), \qquad \text{given} \quad u(0) = u_0, \qquad x \in \mathbb{R}. \tag{1.1}$$

For the most part we understand the noise in the Itô sense although we do also consider the Stratonovich case. For ease of exposition we take $u : \mathbb{R} \times \mathbb{R}_+ \to \mathbb{R}$ although the obvious extensions to higher dimensions hold. For additive noise the function g is taken as a constant whereas for multiplicative noise g depends on u. In the case of no noise ($g = 0$) we recover the deterministic PDE

$$u_t = u_{xx} + f(u), \qquad \text{given} \quad u(0) = u_0, \qquad x \in \mathbb{R}. \tag{1.2}$$

In the deterministic case the analysis of travelling waves both analytically and by numerics is a mature field. This is not the case for SPDEs where much of the analysis is performed for specific equations or for the case of small noise. Indeed with stochastic forcing existence for all time of these waves is not guaranteed and the definition of quantities such as wave speed vary from system to system. For the case of additive noise the position of a stochastic travelling wave is generally determined from the position of a level set. The centres of these fronts can be shown, for small noise, to follow a rescaled Brownian motion, see [25, 7, 12] and in these small noise cases equations can be obtained for the mean wave speed. In the case of multiplicative noise the front may exist for all times and the wave front may have compact support and be well–defined over some time varying interval in space $[a(t), b(t)]$. Multiplicative noise is seen to change the wave speed of the wave and the position is seen to diffuse from the mean (or Goldstein mode), for reviews see [14, 20]. However, it is not our aim to replicate these results here. Instead we develop a new computational technique for computing time dependent waves that may be applied to stochastically forced PDEs.

We extend a numerical method introduced in [5] for deterministic PDEs of the form (1.2) This method freezes the wave in the computational domain by adding a convection term to the equation to compensate for the movement of the wave or pulse. Unlike many ad-hoc methods, where the amount of convection is simply estimated or guessed at, an extra algebraic condition is added to the system and a wave speed is explicitly solved for as a time dependent quantity. To determine the unknown instantaneous wave speed we minimize the L^2 distance between the computed solution and a given fixed template function $\hat{u}$. Convergence of this method for PDEs was considered in [28] and stability of the discrete waves was shown under the same conditions that

*Department of Mathematics and Maxwell Institute, Heriot-Watt University, Edinburgh, EH4 1ER, UK, g.j.lord@hw.ac.uk

†Universität Bielefeld,Bielefeld, Germany, thuemmle@math.uni-bielefeld.de

ensure stability of the continuous solution in [29]. We use this approach to motivate a definition of a stochastic travelling wave. Numerically we solve for the wave profile and a time dependent wave speed for (1.1) which is, in the case of stochastic forcing, a random variable. As a specific example to illustrate the computational method and to compare against existing techniques we consider the scalar Nagumo equation [15]

$$du = [u_{xx} + u(1-u)(u-\alpha)]\,dt + (\nu + \mu u(1-u))dW, \tag{1.3}$$

With $\nu \neq 0$ and $\mu = 0$ we have additive noise and $\mu \neq 0$ the noise is multiplicative. For multiplicative noise we have that $u = 0$ and $u = 1$ are stationary and numerical simulations suggest a wave exists between them. The deterministic equation

$$u_t = u_{xx} + u(1-u)(u-\alpha), \quad u(x,t) \in \mathbb{R},\ x \in \mathbb{R},\ t > 0, \tag{1.4}$$

is often used for testing algorithms since a travelling wave solution $u(x,t) = u_{\rm det}(x-ct)$ connecting the stationary points $u_- = 0$, $u_+ = 1$ of this equation is explicitly known

$$u_{\rm det}(x) = \left(1 + \mathrm{e}^{\frac{-x}{\sqrt{2}}}\right)^{-1}, \quad c = -\sqrt{2}\,(\tfrac{1}{2} - \alpha) \qquad \alpha \in (0, \frac{1}{2}), \tag{1.5}$$

besides other explicit solutions, such as pulses, sources and sinks [8], [1].

In the cases we consider here we discretize the SPDEs and stochastic partial differential algebraic equations(SPDAEs) in space using standard uniformly spaced finite differences and eliminate the boundary conditions. That is for the second derivative with N points and spatial step Δx we approximate the derivative $\partial_{xx} \approx A$ where $A = \frac{1}{\Delta x^2} B \in \mathbb{R}^{N-2,N-2}$ for Dirichlet boundary conditions and for Neumann boundary conditions,

$$A = \frac{1}{\Delta x^2}\begin{pmatrix} -2 & 2 & & \\ & B & & \\ & & 2 & -2 \end{pmatrix} \in \mathbb{R}^{N,N}, \qquad \text{with} \qquad B = \begin{pmatrix} -2 & 1 & & \\ 1 & \ddots & \ddots & \\ & \ddots & \ddots & 1 \\ & & 1 & -2 \end{pmatrix}.$$

For the first spatial derivative $\partial_x \approx 1/\Delta x D_*$ where $* \in \{L, C, R\}$ we introduce

$$D_C = \frac{1}{2}\begin{pmatrix} 0 & a_{1,2} & & \\ -1 & 0 & \ddots & \\ & \ddots & & 1 \\ & & a_{N-1,N} & 0 \end{pmatrix}, D_L = \begin{pmatrix} 1 & & & \\ -1 & 1 & & \\ & \ddots & \ddots & \\ & & -1 & 1 \end{pmatrix}, D_R = \begin{pmatrix} -1 & & & \\ 1 & -1 & & \\ & \ddots & \ddots & \\ & & 1 & -1 \end{pmatrix}$$

and the boundary conditions are dealt with in the standard manner. For convection terms we either used D_C or, where up-winding is an issue, we choose the appropriate D_L, D_R or a weighted combination [5]

$$\partial_x \approx D_\mu := \mathrm{e}^{-\beta\mu} D_L + (1 - \mathrm{e}^{-\beta\mu}) D_R, \tag{1.6}$$

where β is a parameter ($\beta = 0$ or $\beta = \frac{1}{2}$ in our computations) and in what follows μ will be some function of the wave speed.

The outline of the rest of the paper is as follows. We review in Section 2 the computation of travelling waves in the deterministic case and then extend to the case of stochastic forcing. We propose a definition of a stochastic travelling wave based on the deterministic case. We obtain a system of stochastic partial differential algebraic equations (SPDAEs) which we then discretize. In Section 3 we illustrate the numerical method on the Nagumo equation with multiplicative noise and examine numerically (weak) convergence of the profiles and wave speeds of the SPDAE to the SPDE. We investigate the effect of the choice of template function $\hat{u}$ and initial data u^0. In Section 3.2 we present numerical results for Itô and Stratonovich multiplicative noise on how

the wave speed changes with noise intensity. Additive noise in considered in Section 3.3 where we again examine the wave speed with noise intensity and illustrate the algorithm when new travelling waves are nucleated. Finally we consider weaker versions of the stochastic travelling wave fixed in the computational domain by mean wave speeds and then discuss the results and computational method.

2. Freezing travelling waves. In this section we introduce the (stochastic) differential algebraic equations that we use to define the travelling wave problem. We start by reviewing the more familiar deterministic case before considering the case with stochastic forcing. In both cases we reduce the infinite problem to finite dimensions by truncating the computational domain and discretizing in space.

2.1. Deterministic PDE. Let us assume that equation (1.2) has a travelling wave solution u, so that u can be written as

$$u(x,t) = u_{\text{det}}(\xi), \quad \xi = x - \lambda_{\text{det}} t, \tag{2.1}$$

where $u_{\text{det}} \in \mathcal{C}_b^2(\mathbb{R}, \mathbb{R}^m)$ denotes the waveform and λ_{det} its wave speed. In a comoving frame $v(\xi,t) = u(\xi - \lambda_{\text{det}} t, t)$ equation (1.2) reads

$$v_t = v_{\xi\xi} + \lambda_{\text{det}} v_\xi + f(v), \quad \xi \in \mathbb{R}, \quad t \geq 0 \tag{2.2}$$

of which the travelling wave u_{det} is a stationary solution. Since the wave speed λ_{det} is generally unknown we transform equation (1.2) into a co-moving frame with unknown position $\gamma(t)$, i.e. we insert the ansatz $v(x,t) = u(x - \gamma(t), t)$ into (1.2). Then we obtain

$$v_t = v_{xx} + f(v) + \lambda v_x, \tag{2.3}$$

where $\lambda(t) = \gamma'(t)$. In order to compensate for the additional variable λ we add a so called phase condition

$$0 = \psi(v, \lambda) \tag{2.4}$$

which together with (2.3) forms a partial differential algebraic equation (PDAE) [5]. The position γ of the wave can then be calculated by integrating

$$\gamma' = \lambda, \quad \gamma(0) = 0, \qquad \text{to get} \qquad \gamma(t) = \int_0^t \lambda(s) ds.$$

For the numerical implementation we need to truncate the spatial domain from $x \in \mathbb{R}$ to $x \in [0, L]$ and impose appropriate boundary conditions such as Neumann, Dirichlet or projection boundary conditions [28]. We then solve (2.3) and (2.4) for $x \in [0, L]$. In contrast to traditional travelling wave computations this method does not rely on λ being a constant wave speed.

2.1.1. Choice of phase condition. Thus far we have not discussed the choice of the phase fixing function ψ in (2.4). Since the phase condition only selects one representative out of the infinite family of solutions, there is some freedom of choice here. The simplest phase condition is to align to some norm the solution with respect to a given template function $\hat{u}$, that is we minimize the $\|u - \hat{u}\|$ for a given norm. It is natural to take the L^2 norm in which case we take

$$\psi_{\text{fix}}(u) = \langle \hat{u}_x, u - \hat{u} \rangle.$$

This choice was termed the template fitting method in [23]. Clearly there is a choice as to the profile to minimize against. By using this phase condition the PDAE defined by (2.4), (2.3) is of differentiation index 2. It is possible to reduce the index by differentiating (2.4) with respect to time to obtain

$$\psi_{\text{fix,diff}}(u, \lambda) = \langle \hat{u}_x, u_t \rangle = \langle \hat{u}_x, u_{xx} + f(u, u_x) + \lambda u_x \rangle.$$

Another possible choice of phase condition stems from minimizing the temporal change $\|v_t\|_{L^2}$ and this leads to the orthogonality constraint, also known as the method of mechanical connections [23] in the deterministic case:

$$\psi_{\text{orth}}(u) = \langle u_x, u_t \rangle.$$

The last two techniques are applicable where the solution is differentiable in time and so in general apply only to the deterministic system [5].

2.1.2. Discretization. Discretizing in space with N grid points and after eliminating the boundary conditions we obtain the following DAE system for $\lambda \in \mathbb{R}$ and $v \in \mathbb{R}^{N-2}$ for Dirichlet or $v \in \mathbb{R}^N$ for Neumann boundary conditions

$$\begin{aligned} v' &= Av + \lambda(D_\lambda v + \eta) + f(v) + \varphi \\ 0 &= \psi^h(v, \lambda), \end{aligned} \tag{2.5}$$

where the vectors φ, η are used to deal with the boundary conditions. This system can be solved by using appropriate DAE solvers [3] or we can use a linear implicit Euler method to obtain the fully discrete system

$$\begin{aligned} v^{n+1} &= v^n + \Delta t \left[Av^{n+1} + \lambda^{n+1}(D_{\lambda^n} v^n + \eta) + f(v^n) + \varphi \right] \\ 0 &= \langle D_C \hat{u}, v^{n+1} - \hat{u} \rangle \end{aligned} \tag{2.6}$$

which leads to the system

$$\begin{pmatrix} I - \Delta t A & -\Delta t(D_{\lambda^n} v^n + \eta) \\ \Delta x\, D_C \hat{u}^T & 0 \end{pmatrix} \begin{pmatrix} v^{n+1} \\ \lambda^{n+1} \end{pmatrix} = \begin{pmatrix} \Delta t(v^n + f(v^n) + \varphi) \\ \langle D_C \hat{u}, \hat{u} \rangle \end{pmatrix}.$$

Note that for the reference or template $\hat{u}_x$ we use the central difference approximation D_C since this is most accurate and is convection instabilities are not an issue for this term.

It has been shown in [28] that for $L \to \infty$ and $\Delta x \to 0$ the stationary solution of (2.5) converges to the exact travelling wave solution of the PDE (under a uniqueness assumption). Moreover it has been shown that the solution of (2.5) inherits the nonlinear stability properties of (1.2).

2.2. Stochastic PDE and stochastic travelling wave. We seek travelling wave solutions to the SPDE

$$du = [u_{xx} + f(u)]\, dt + g(u) dW, \quad u(0) = u^0 \tag{2.7}$$

posed on the real line with $g(u) = (\nu + \mu h(u))$, where ν and μ are parameters that allow us to consider additive and multiplicative noise. We consider noise given by $W(t)$, a Q–Wiener process [11], and assume that Q has eigenfunctions ϕ_n with corresponding eigenvalues $\zeta_n \geq 0$, in which case

$$W(t) = \sum_n \zeta_n^{1/2} \phi_n \beta_n(t), \tag{2.8}$$

for independent Brownian motions β_n. We assume that the covariance Q operator of $W(t)$ satisfies either $Q = I$ and we have space-time white noise or that we approximate exponential decay in the correlation length $\xi > 0$ in which case

$$\mathbb{E}\left(W(t,x)\right)\mathbb{E}\left(W(s,y)\right) \approx \min(t,s) Q(x-y), \qquad Q(x) = \frac{1}{2\xi} \exp\left(-\frac{\pi x^2}{4\xi^2}\right),$$

$\zeta_n = \exp(-\frac{\xi^2 \lambda_n}{L})$, where $\lambda_n = \frac{n^2\pi^2}{L^2}$ where L is the length of the interval [26, 17]. Results on the existence of a solution for (2.7) on the infinite domain can be found in [31] with f and g Lipschitz

and further results maybe found in [11, 9]. Other results exists for the Allen-Cahn equation with additive noise see [22] and for the stochastic FKPP equation [27].

Although intuitively it is understood what is meant by a stochastic travelling wave it is not easy to find a definition in the literature, however for a review see [14]. Typically a stochastic travelling wave and speed is either defined by the evolution of a level set such as in [19, 30] or through the evolution relative to a deterministic wave, such as through a small noise expansion such as in [18]. Inspired by the deterministic fixing of a wave we define a stochastic travelling wave relative to a reference function $\hat{u}$ and consider the following SPDAE for $(v(x,t),\lambda(t))$

$$\begin{aligned} dv &= \left[v_{xx} + \lambda v_x + f(v)\right] dt + g(v) dW, \quad v(0) = u^0 \\ 0 &= \psi(v,\lambda). \end{aligned} \tag{2.9}$$

We define u to be a travelling wave solution of the SPDE (2.7) with respect to template function $\hat{u}(x)$ if there exists a random variable λ such that v satisfies (2.9) and $\|v-\hat{u}\|_{L^2}$ is minimized, and

$$u(x,t) = v\left(x - \int_0^t \lambda(s) ds, t\right).$$

We call the time-dependent random variable $\lambda(t)$ the instantaneous wave speed and the time-average

$$\Lambda(t) := \frac{1}{t}\int_0^t \lambda(s) ds$$

the wave speed at time t. If we minimize the distance in the L^2 norm then once again the natural phase condition for (2.9) is

$$\psi(u,\lambda) = \langle \hat{u}_x, u - \hat{u}\rangle = 0.$$

We are not going to perform a convergence analysis here of the SPDAE. However, we note that for the case of small noise we can apply Itô's lemma and perform standard analysis to obtain a modified deterministic PDE to which the results of [28] may be applied to relate the solutions of the SPDE to the SPDAE.

By defining a travelling wave through (2.9) we introduce the random variable λ (which we called instantaneous wave speed) which is used to freeze the wave. We could instead define a weaker versions by taking statistics of λ. For example we can take the time-averaged wave speed $\Lambda(t)$ for each realization

$$\begin{aligned} dv &= \left[v_{xx} + \Lambda v_x + f(v)\right] dt + g(v) dW, \quad v(0) = u^0 \\ 0 &= \psi(v,\lambda). \end{aligned} \tag{2.10}$$

Other weaker forms of travelling wave solution are possible where the instantaneous wave speed λ or time average wave speed Λ of an individual realization is replaced by its expectation over realizations

$$\begin{aligned} dv &= \left[v_{xx} + \mathbb{E}(\lambda) v_x + f(v)\right] dt + g(v) dW, \quad v(0) = u^0 \\ 0 &= \psi(v,\lambda); \end{aligned} \tag{2.11}$$

and

$$\begin{aligned} dv &= \left[v_{xx} + \mathbb{E}(\Lambda) v_x + f(v)\right] dt + g(v) dW, \quad v(0) = u^0 \\ 0 &= \psi(v,\lambda). \end{aligned} \tag{2.12}$$

Using the sample mean of λ and Λ for fixing we are essentially using a "group velocity" to fix the wave and as a result the mean profile will contain a spread as each individual realization is not fixed at the same point. By taking these weaker notions of wave speed to freeze" the wave we observe spreading of the front profiles, as discussed in [14], (see for example Figure 3.13).

So far we have not commented on the choice of profile $\hat{u}$ to minimize against. The obvious choice is to minimize against the profile of the unforced travelling wave from the deterministic system when such a wave exists. For the stochastic PDE this mimics the small noise type analysis of seeking waves close to the deterministic waves. In examples where we do not have an analytic expression for the deterministic travelling wave $\hat{u}$ then this can be solved for simultaneously or a sample solution solved for and saved. However, this is a matter of choice and we could minimize the L^2 norm against any fixed profile. The other obvious choice for a template function is to ask for the wave speed and profile with respect to the given initial data u^0. We examine these different choices of template functions $\hat{u}$ in the numerical results in Section 3.

2.2.1. Discretization of the SPDAEs. We truncate (2.7) and (2.9) to a finite domain with $x \in [0, L]$ and impose either Dirichlet or Neumann boundary conditions at $x = 0$ and $x = L$. We discretize the derivatives in space by the finite differences approximations outlined in Section 1. For our time discretizations we consider here the semi–implicit Euler–Maruyama methods for Itô noise and the Heun method to approximate Stratonovich noise, see for example [16]. To discretize the noise we need to implement a Brownian increment ΔW_n. For space–time white noise we can take the jth element of ΔW_n as $\sqrt{\frac{\Delta t}{\Delta x}}\ \chi_n$ where χ_n are normally independent identically distributed with mean zero and variance one. For spatially correlated (smoother) noise we use the eigenfunctions of the linear operator to form the noise using (2.8) and evaluate on the finite difference grid on $[0, L]$.

The linear semi–implicit Euler–Maruyama scheme gives the discretization

$$\begin{aligned} u^{n+1} &= u^n + \Delta t \left[A u^{n+1} + \lambda^{n+1} \left(D_{\lambda^n} u^n + \eta \right) + f(u^n) + \varphi \right] + g(u^n) \Delta W_n \\ 0 &= \langle \hat{u}_x, u^{n+1} - \hat{u} \rangle \end{aligned} \tag{2.13}$$

and given u^n (and λ^n) we can solve (2.13) to find u^{n+1} and λ^{n+1} at the cost of an extra linear solve

$$\begin{pmatrix} I - \Delta t A & -\Delta t (D_{\lambda^n} v^n + \eta) \\ \Delta x\, D_C \hat{u}^T & 0 \end{pmatrix} \begin{pmatrix} v^{n+1} \\ \lambda^{n+1} \end{pmatrix} = \begin{pmatrix} \Delta t (v^n + f(v^n) + \varphi) + g(u^n) \Delta W_n \\ \langle D_C \hat{u}, \hat{u} \rangle \end{pmatrix}.$$

This scheme has better stability properties than solving (2.13). The weaker versions of the stochastic travelling wave systems (2.10), (2.11) and (2.12) are discretized and solved for in a similar way.

In order to deal with the Stratonovich noise we use the explicit Euler - Heun method [13, 16]

$$\begin{aligned} z &= u^n + g(u^n) \Delta W_n \\ u^{n+1} &= u^n + \Delta t \left[A u^n + \lambda^n \left(D_{\lambda^n} u^n + \eta \right) + f(u^n) + \varphi \right] + \frac{1}{2} (g(z) + g(u^n)) \Delta W_n \\ 0 &= \langle \hat{u}_x, u^{n+1} - \hat{u} \rangle. \end{aligned} \tag{2.14}$$

The literature on solving stochastic DAEs is in its infancy, however there are some analytic and computational results mainly arising from examining noise in circuit simulations, see for example [24, 21, 32, 33].

3. Numerical Results. We use the Nagumo equation (1.3) to illustrate the algorithm for both multiplicative and additive space-time white noise. We solve (2.9) using the linear implicit method (2.6) with Dirichlet boundary conditions and the following numerical parameters: $L = 60, \Delta x = 0.5, \Delta t = 0.1$.

We compare beloa wave speeds and profiles where the wave is fixed from solving the SPDAE (2.9) and from solving the SPDE (2.7) directly. Wave Speeds for the SPDAE are computed from random variable λ and we consider

$$\mathbb{E}(\lambda), \qquad \Lambda(t) = \frac{1}{t} \int_0^t \lambda(s) ds, \qquad \mathbb{E}(\Lambda), \qquad \bar{\Lambda} = \frac{1}{T_2 - T_1} \int_{T_1}^{T_2} \mathbb{E}(\Lambda(t))\, dt. \tag{3.1}$$

We approximate the integrals over time for $\Lambda(t)$ and $\bar{\Lambda}$ above by the trapezoidal rule.

$\bar{\Lambda}$	$\mu = 0$	$\mu = 0.0625$	$\mu = 0.125$	$\mu = 0.25$	$\mu = 0.5$	$\mu = 1$
$N = 1000$	0.35344	0.35354	0.35380	0.35476	0.35874	0.37660
$N = 10000$		0.35353	0.35377	0.35462	0.35853	0.36578

TABLE 3.1

Limiting wave speeds $\bar{\Lambda}$ as a function of noise intensity μ with $\hat{u} = u_0 = u_{\text{det}}$ and the expectation taken over 1000 and 10000 realizations and $T_1 = 100, T_2 = 200$. Note the value for $\mu = 0$ is a computed value, where as the analytic value is $\sqrt{2}/4 \approx 0.35355$.

For the SPDE with a well defined wave with compact support so that at $u(-\infty, \cdot) = u_-$, $u(\infty, \cdot) = u_+$ we can define a travelling wave and wave speed using the two points

$$a(t) := \sup\{z : u(x,t) = u_-, x \le z\}, \quad b(t) := \sup\{z : u(x,t) = u_+, x \ge z\}, \tag{3.2}$$

and in addition we can take the 'mid point' level set of a wave

$$c(t) := \sup\{z : u(x,t) = (u_- + u_+)/2, x \le z\}. \tag{3.3}$$

For some realizations of the SPDAE below we need to deal with solutions that fail to exists after some finite time. To do this we can either monitor the instantaneous wave speed so that $|\lambda(t)| < tol$ or the L^2 norm $\|u(t)\|_{L^2} < tol$ for some tolerance tol (which we took to be 10).

3.1. Multiplicative noise. We present numerical results with $\alpha = 0.25$ for the nonlinearity in the computation of v and λ for (1.3) with $\nu = 0$. The majority of the results are performed with 1000 realizations, however we also examine a larger sample of 10000 realizations. We examine different values for the intensity of the noise but in particular we take $\mu = 0.5$ to compare the majority of solutions.

3.1.1. A test case. To test the algorithm we use the exact deterministic solution (1.5) for both the initial value ($u^0 = u_{\text{det}}$) and for the template function ($\hat{u} = u_{\text{det}}$). In Figure 3.1 (a) we plot in space-time a single realization of the travelling wave fixed in the computational domain. There is an interface at $x \approx 30$ which does not travel as we integrate in time, illustrating a single realization is frozen by the algorithm (compare to Figure 3.3 where the wave is not fixed). The instantaneous wave speed $\lambda(t)$ used to the fix the wave is plotted in (b). In (c) we plot the wave speed $\Lambda(t)$ computed from the instantaneous wave speed $\lambda(t)$ in (b). In this realization we observe an initial transient in $\Lambda(t)$ before convergence to a well defined quantity. In Figure 3.2 we show mean profiles and mean wave speeds over different realizations of the same system. In (a) the mean (over 1000 samples) of the solution v at $T_2 = 200$ is displayed. In Figure 3.2 (b) and (c) we plot the $\mathbb{E}(\lambda)$ and $\mathbb{E}(\Lambda)$ respectively over 1000 realizations and 10000 realizations. These two plots illustrate the variability in the mean instantaneous wave speeds $\mathbb{E}(\lambda)$ and convergence of the time average wave speed $\mathbb{E}(\Lambda)$ to a well defined quantity. We can get an estimate of limiting wave speed $\bar{\Lambda}$, for example taking $T_1 = 100$ and $T_2 = 200$. For $\mu = 0.5$ we find $\bar{\Lambda} \approx 0.3587$ and $\bar{\Lambda} \approx 0.3585$, (with 1000 and 10000 realizations) this compares with the deterministic wave speed of 0.3534. For the profiles of the computed waves we have that at $T_2 = 200$ the L^2 difference between the mean profile and the deterministic profile is in the order of 10^{-3} for 1000 as well as for 10000 samples.

To provide some validation of the computations with the SPDAE we compare profiles and wave speeds from direct simulation of the SPDE (2.7). In Figure 3.3 (a) is plotted the solution from a single realization and in contrast to Figure 3.1 (a) we see the interface propagate in time to the right, in Figure 3.3 (b) we show the mean profiles at $t = 0$, $t = 500$, $t = 1000$ and $t = 2000$. Since the wave now propagates we are forced to consider a much larger computational domain. In Figure 3.4 (a) we show mean wave speeds from such a computation. We compare the value obtained from the wave speed $\bar{\Lambda}$ with the corresponding values $a(t)/t$, $b(t)/t$, $c(t)/t$ used to define the wave speed using a direct simulation of the travelling wave defined in (3.2) and (3.3). The values of $a(t)/t$, $b(t)/t$, $c(t)/t$ converge slowly to the limiting value $\bar{\Lambda}$ obtained with the freezing approach. In fact we observed that the convergence of $\Lambda(t)$ in general is much faster

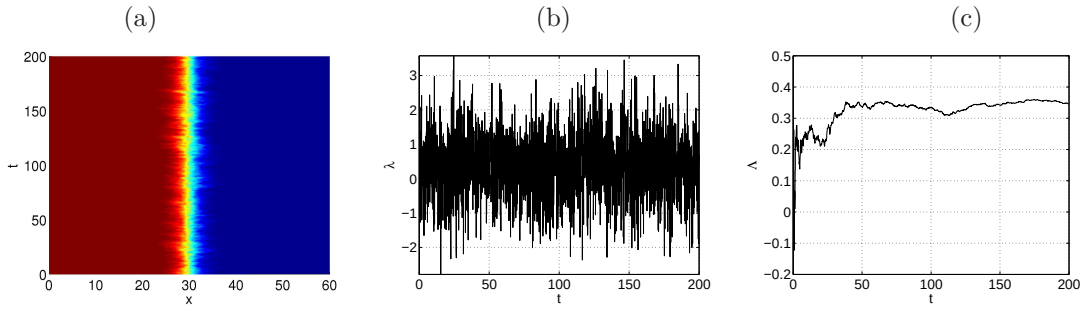

FIG. 3.1. *(a) Space-time plot of a single realization, frozen using SPDAE (2.9), in (b) the corresponding instantaneous wave speed $\lambda(t)$, and in (c) the wave speed $\Lambda(t)$.*

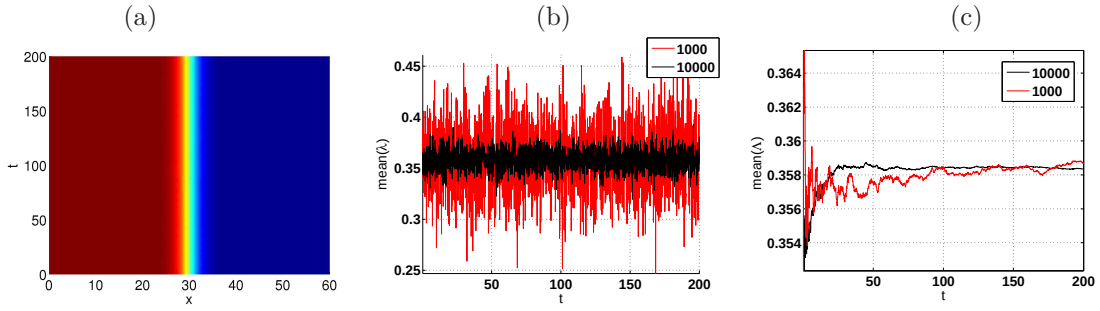

FIG. 3.2. *Plot of mean profile (a) over* 1000 *realizations, (b) the mean instantaneous wave speeds, $\mathbb{E}(\lambda(t))$ and (c) wave speeds $\mathbb{E}(\Lambda(t))$ with* 1000 *and* 10000 *realizations.*

than $a(t)/t,\ b(t)/t,\ c(t)/t$ By data fitting with $X(t) = \alpha/t + \beta,\ X \in \{a, b, c\}$ and extrapolation we obtained limiting values of $a \approx 0.3413$, $b \approx 0.34134$ and $c \approx 0.34123$.

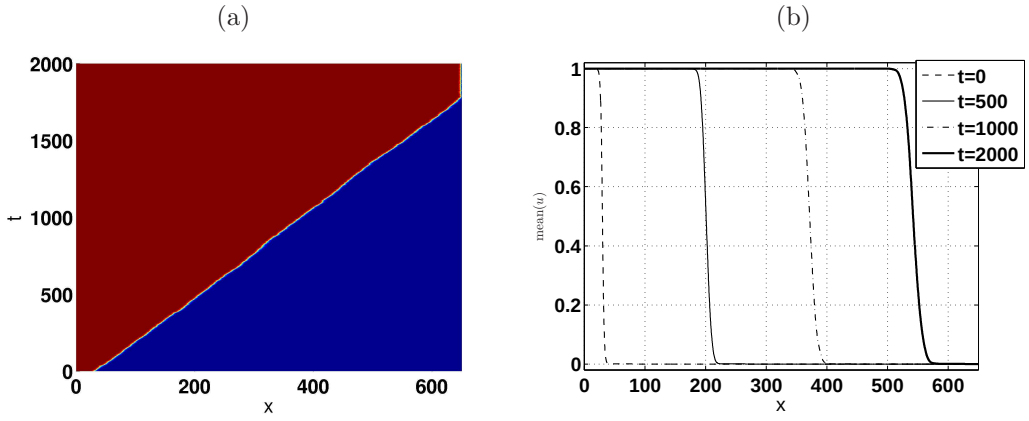

FIG. 3.3. *(a) Space-time plot of a single realization solved with no freezing. In (b) are plotted snapshots of mean(u) for travelling wave at $t = 0$, $t = 500$, $t = 1000$ and $t = 2000$.*

We also compare the mean profiles from the SPDE to the profile obtained from the SPDAE. To avoid the spreading of the wave we align all the SPDE solutions by taking the level set $c(200)$ as a common reference. In the absence of noise the L^2 error is of order 10^{-6}. In Figure 3.4 (b) the weak error

$$\|\mathbb{E}(u_{SPDAE}) - \mathbb{E}(u_{SPDE})\|_{L^2}^2$$

is plotted against time, where the expectation is taken over 1000 realizations. We see that the

differences between the mean profiles increases with the noise but that it remains small. This is a good indication that the profiles computed by the two methods are the same.

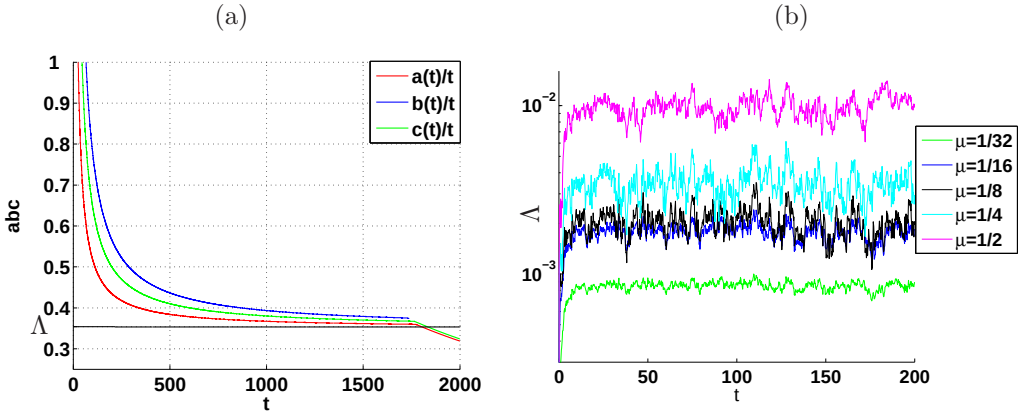

FIG. 3.4. *In (a) we have plotted mean wave speeds $a(t)/t, b(t)/t,\ c(t)/t$ via a level set approach, note the slow convergence to $\bar{\Lambda}$ of the SPDAE and the effect of the boundary for $t > 1750$. In (b) a comparison of the L^2 weak error between the SPDE (2.7) and SPDAE (2.9) in time as the strength of the noise increases.*

Remark: Extrapolation of a, b and c to obtain a limiting value of approximately 0.341 from the SPDE leads to and underestimate if we compare $\bar{\Lambda} = 0.3544$ ($\mu = 0.5$ from Table 3.1.1) from the SPDAE. A similar phenomena is seen in the deterministic setting ($\mu = 0$) where a, b and c are also slow to converge and implicit Euler with a large step size also gives an underestimate of the wave speed. Solving the PDE using implicit Euler for $\Delta t = 0.01$ we find a wave speed of $\Lambda \approx 0.3531$ and for $\Delta t = 0.1$ $\Lambda \approx 0.3501$ (based on the position of $c(t)$). If we freeze the wave wave we obtain $\Lambda \approx 0.35344$ for $\Delta t = 0.1$ and $\Delta t = 0.01$. The analytic value for the deterministic travelling wave on the real line is $\bar{\Lambda} = \sqrt{2}/4 \approx 0.35355$.

3.1.2. Choice of reference $\hat{u}$. Now that we have tested the SPDAE approach we now examine the sensitivity of the algorithm to the choice of the template function $\hat{u}$. We tested the algorithm with a range of different template functions: a perturbation of the deterministic solution $\hat{u} = u_{pd}$ was chosen so as not to satisfy the boundary conditions as $u_{pd}(0) = 0.8$ and $u_{pd}(L) = 0.2$. The other template functions all satisfy the boundary conditions ($u_{\surd}, u_{\tanh}, u_{\text{lin}}$ and $u_{\cos}$) but with different profiles

$$u_{pd} = 0.6/(1+\exp(x-L/2))+0.2, \qquad u_{\surd} = \frac{1}{2}+\frac{L-2x}{\sqrt{2+L-2x^2}}, \qquad u_{\tanh} = (1+\tanh(L/2-x))/2$$

$$u_{lin}(x) = (L-x)/L, \qquad u_{\cos}(x) = \cos(\pi x/L).$$

In the deterministic setting, all these template functions lead to well defined profiles and wave speeds. In Figure 3.5 $\mathbb{E}\Lambda(t)$ is plotted with $\hat{u} \in \{u_{pd}, u_{lin}, u_{\tanh}, u_{\surd}\}$ as template functions for $\mu = 0.00626$ (a), $\mu = 0.25$ (b)and $\mu = 0.5$ (c). For all these values the wave speeds follow the same trend in t and appear to converge, however closer inspection suggests that for $\hat{u} = u_{\text{lin}}$ we obtain a systematically smaller wave speed (more evident as the noise intensity is increased). To get estimates of the limiting wave speeds we take $T_1 = 100$ and $T_2 = 200$ and base or expectation on those solutions that exist to $T_2 = 200$, the results are shown in Table 3.1.2. Comparing to Table 3.1.1 we see the same qualitative behaviour as μ is increased and for $\mu = 0.5$ a limiting value of $\bar{\Lambda} \approx 0.36$. The consistently low estimate for the wave speed using $\hat{u} = u_{lin}$ is observed for finer discretization and changing the parameter β in the convection term. Note that for the larger noise $\mu = 0.5$ some of our realizations fail to exist (the wave speed becomes numerically unbounded) and the minimization of the L^2 norm has failed. For the SPDE and the SPDAE with the reference function $\hat{u} = u_{\text{det}}$ of Section 3.1.1 we do not observe this spurious behaviour. These

$\hat{u}$	u_{pd}	u_{lin}	$u_{\surd}$	$u_{\tanh}$
$\mu = 0.00625$	0.3532	0.3532	0.3531	0.3533
$\mu = 0.125$	0.3535	0.3533	0.3533	0.3536
$\mu = 0.25$	0.3546	0.3537	0.3544	0.3551
$\mu = 0.5$	0.3594 (999)	0.3551	0.3583 (592)	0.3604 (535)

TABLE 3.2

Limiting wave speeds $\bar{\Lambda}$ as a function of noise intensity and reference functions $\hat{u}$, with $T_1 = 100$, $T_2 = 200$ and 1000 realizations. For $\mu = 0.5$ we indicate the number of samples where that is less than 1000.

failures are based on the choice of the reference function and arise from the discretization of the convection term, see the discussion in Section 4. For the template $\hat{u} = u_{\cos}$ we have a large number of realizations that fail to exist and very slow convergence of the wave speed.

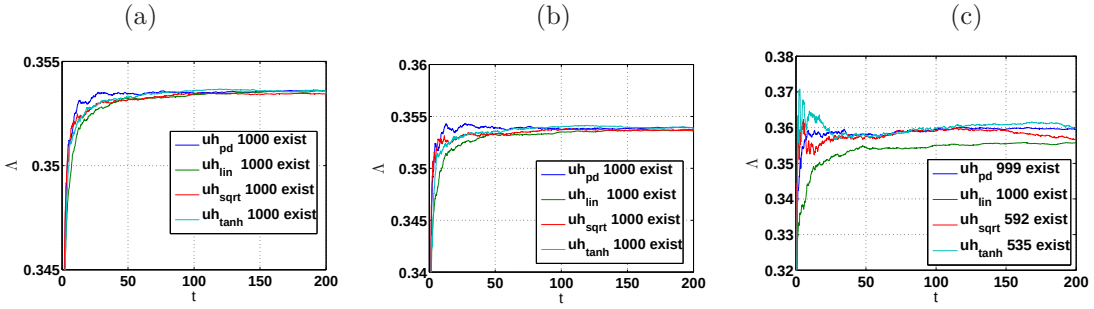

FIG. 3.5. *Plot of $\mathbb{E}(\Lambda(t))$ for different choices of references $\hat{u}$ (a) $\mu = 0.0625$, (b) $\mu = 0.125$ and (c) $\mu = 0.5$ where the mean is taken over solutions that exist to time $T = 200$.*

3.1.3. Sensitivity to the choice of initial data. We now examine convergence in the initial data u^0 with a template function of $\hat{u} = u_{\det}$. Starting the SPDAE computations of the travelling wave with the linear function $u^0 = u_{\lin}$ gives different results. There is now a transient time to converge to the travelling wave. This is illustrated in Figure 3.6 where we have plotted the evolution of the mean wave profile in (a) of the SPDAE with 1000 realizations and in (b) one realization from the SPDAE. In both (a) and (b) after an initial transient, the wave is fixed, compare to (c) which shows one sample from solving the SPDE.

During the transient when the wave is fixed many of the realizations fail due to the fact that λ gets too large – and so the minimization of the L^2 norm fails. We consider these as the wave ceasing to exist (and these are removed before taking the mean). We assume that in this case these failures are purely due to the large convection since for the SPDE all realizations converge to a travelling wave form. By monitoring the wave speed we are able to determine the extinction time of the travelling wave.

In Figure 3.7 we show the time averaged mean of λ with respect to realizations where $|\lambda| < 10$ as well as their number N_{exist}. In (a) we show $\mathbb{E}(\lambda)$ and in (b) $\mathbb{E}(\Lambda)$ based both on all solutions and those that only survive to the final time. We observes that N_{exist} decreases from 10000 to 89 during the transitional period exponentially. The spurious extinction of waves during the transient due adding in the convection term and the associated numerical instabilities is a disadvantage of the method as implemented.

3.1.4. Spatially correlated noise. We can examine the performance of the method for noise with different spatial correlations - in particular as the spatial regularity of the noise increases. Solutions are similar to the space–time white noise cases such as Figure 3.1 and Figure 3.2 and are not reproduced here.

In Figure 3.8 (a) we have plotted the mean wave speed $\Lambda(t)$ against time for three different correlation lengths $\xi = 1, 10, 100$ and with two different reference functions $\hat{u} = u_{det}$ and $\hat{u} = u_{lin}$. First consider the reference function $\hat{u} = u_{det}$. We see that the effect of increasing the correlation

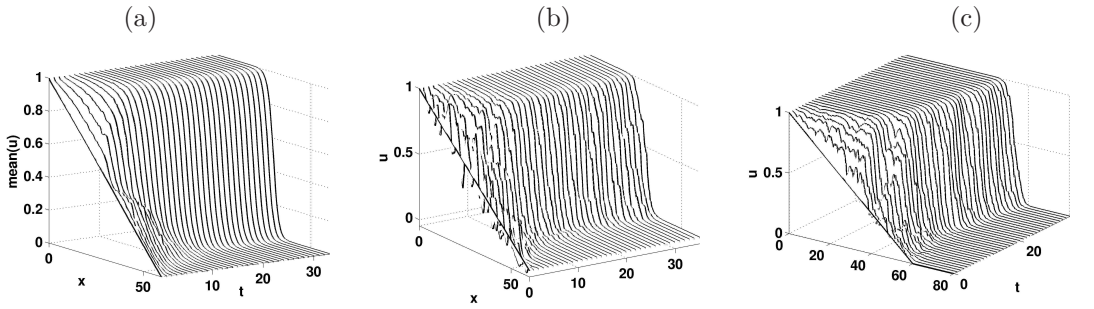

FIG. 3.6. *Solution of the Nagumo equation with initial data $u^0 = u_{lin}$. In (a) the mean and (b) a single realization both computed using the fixing with $\hat{u} = u_{det}$. There is a small transient and the wave remains fixed. In (c) is a single sample where the wave is not fixed in the domain and we see the wave travelling during and after the transient.*

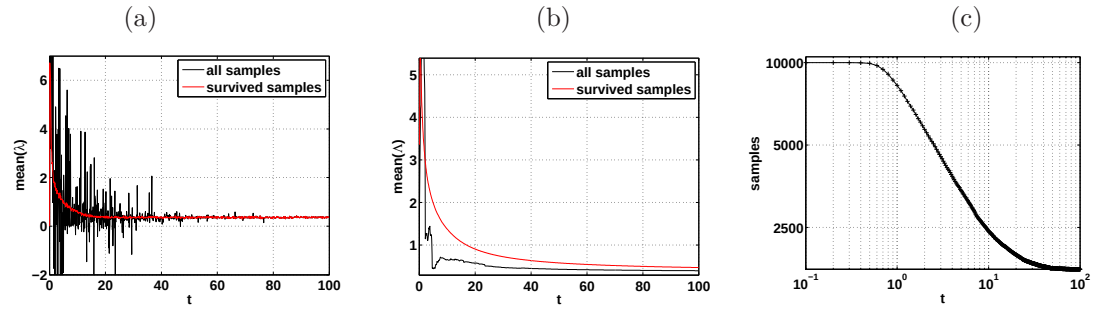

FIG. 3.7. *In (a) we plot $\mathbb{E}(\lambda(t))$ based on all 10000 samples and based on only those that survive to the final time and in (b) is plotted the corresponding $\mathbb{E}(\Lambda)$. Finally we plot the number of solutions that exist as a function of time. After a rapid decrease 89 exist to the final time.*

length is to decrease the wave speed from $\bar{\Lambda} = 0.3591$ for the space-time white noise (see Table 3.1.2). We see a similar drop in the wave speed with correlation length taking $\hat{u} = u_{lin}$ and furthermore for large correlation lengths (spatially smooth noise) the wave speeds for the two different reference functions converges and is close to the deterministic value.

In Figure 3.8 (b) we have examined the effect of the spatial correlation on the existence of solutions in the transient period with initial data $u^0 = u_{lin}$ and now $\hat{u} = u_{det}$. We see that as the noise is smoother in space (as ξ increases) there are fewer solutions that cease to exist due to the numerical instability from the convection term.

3.2. Itô & Stratonovich multiplicative noise. In this section we briefly examine the effect of Itô versus Stratonovich noise on the computed wave speeds. In [2] Stratonovich noise is considered with a correlation length equal to be that of the grid spacing so that $\xi = \Delta x = 0.2$ for a range of different non–linear regimes. We consider a scaled noise intensity and define $\epsilon = \mu^2$ and examine how the wave speed $\bar{\Lambda}$ varies as the noise intensity ϵ is increased. The authors obtain a front velocity from an average over an "appropriate time window" of $\int_L u(x,t)dt$ and compare to a small noise analysis. We use our definition of the travelling wave and our method to compute wave speed against the noise intensity using the Heun method of (2.14). Results are shown in Figure 3.9 (a) for $\alpha \in \{-1, -0.5, -0.3, 0, 0.3, 0.45\}$. To obtain the limiting wave speed the averages are taken over 1000 realizations that exist to a final time of $T_2 = 200$. We recover in the Stratonovich case the well known results that the wave speed increases with the noise intensity. Note that due to waves ceasing to exist in some cases we needed to compute with a large set of initial realizations and for $\alpha = 0.45$ with Stratonovich noise it was not feasible to obtain 1000 realizations for $\epsilon = 0.5$, 0.55 and 0.6 that existed at $T_2 = 200$.

In Figure 3.9 (b) we repeat the calculations however now for Itô noise and we do not observe the same increase in wave speed with the noise intensity. Indeed for the nonlinearity with $\alpha = -1$

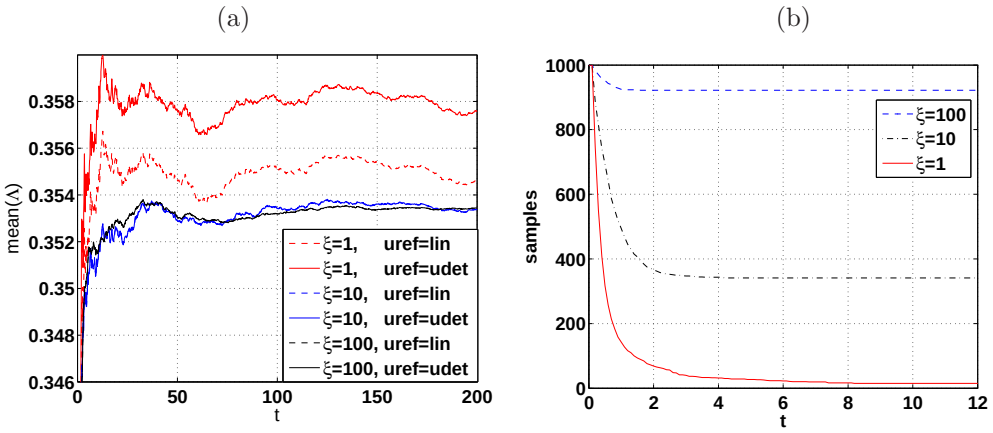

FIG. 3.8. *For spatially correlated noise (a) the dependence of wave speed on the correlation length ξ for two $\hat{u} = u_{det}$ and $\hat{u} = u_{lin}$. In (b) we see that as correlation length is increased the number of samples surviving the transient starting from initial condition $u^0 = u_{lin}$ increases.*

the wave speed is no longer strictly increasing as a function of the noise intensity. Since an Itô–Stratonovich correction changes the non–linear term we would not expect to see exactly the same behaviour for large noise.

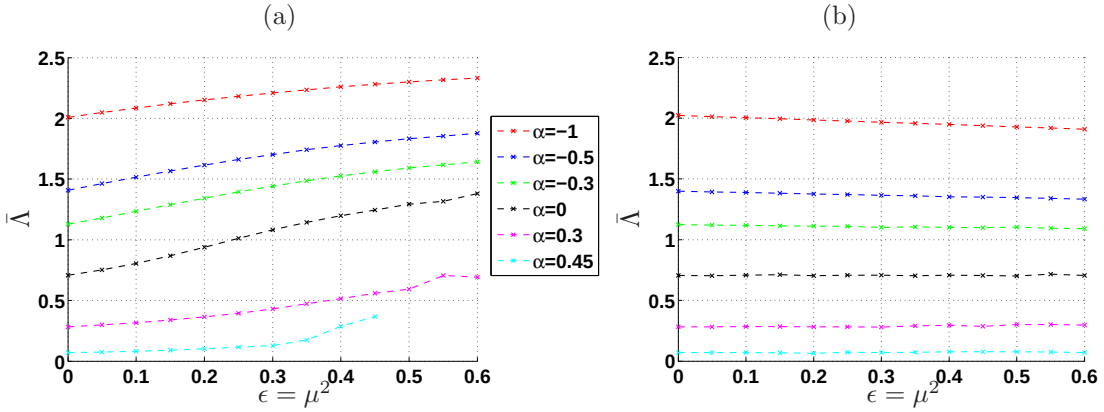

FIG. 3.9. *Wave speeds $\bar{\Lambda}$ with increasing noise intensity for Stratonovich noise (a) and Itô noise (b), each line corresponds to a different nonlinearity with $\alpha \in \{-1, -0.5, -0.3, 0, 0.3, 0.45\}$, each data point taken with* 1000 *realizations and $T_2 = 200$.*

3.3. Additive noise. We briefly consider the case of additive noise in the SPDE for which, unless the noise has some special properties, a solution will in general cease to exist at some finite time. However, even for quite large noise, a wave like structure can persist for long times. We can use our definition to define the travelling wave in this case, where the level set is not well defined, and to determine wave speeds and existence times. First we consider small additive noise i.e. $\nu = 0.05$ and $\mu = 0$. For this case we know from analytical results (eg [7, 12], see also [14]) that the wave front follows a Brownian path. In Figure 3.10 (a) we plot a sample realization and in (b) is plotted the instantaneous wave speed $\lambda(t)$ and in (c) the wave speed $\mathbb{E}(\Lambda(t))$ computed from those solutions that exist at time $T = 200$.

We now change the parameter α in the non-linearity to $\alpha = 0.1$ and illustrate how the SPDAE approach deals with nucleation and extinction of waves. In Figure 3.12 we have plotted in (a) a single realization of the SPDE (so not frozen) showing nucleation and subsequent extinction ($t \approx 98$) of a travelling wave. In (b) is plotted a single realization from computing using the SPDAE approach. We see the wave is fixed in the domain and at $t \approx 50$ a wave is nucleated at

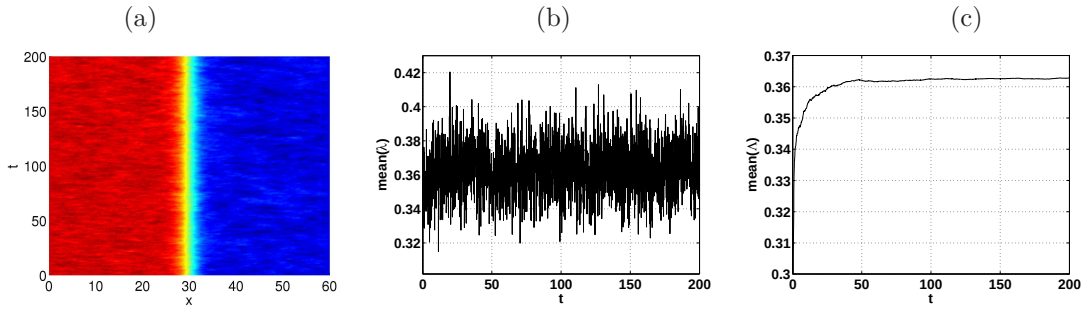

FIG. 3.10. *Additive noise with $\nu = 0.05$. In (a) a sample realization fixed in the domain and in (b) the corresponding $\lambda(t)$. In (c) is plotted the wave speed $\mathbb{E}(\Lambda(t))$.*

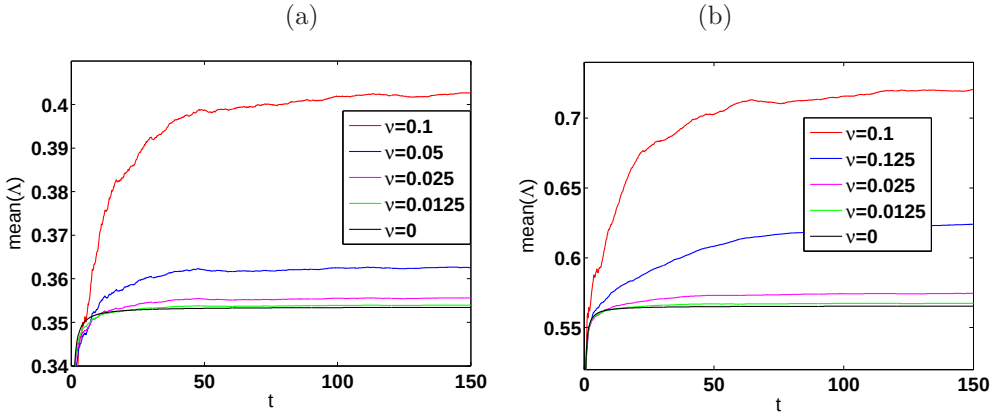

FIG. 3.11. *Influence of additive white noise on the wave speed $\bar{\Lambda}$ for (a) $\alpha = 0.25$ and (b) $\alpha = 0.1$. In both cases there is a clear increase in the wave speed from the deterministic case ($\nu = 0$) as the wave speed is increased.*

$x \approx 100$ by the additive noise. The computations are based on the original wave which remains fixed until it interacts with the nucleated wave and is annihilated at $t \approx 94$ when the computations stop when the wave cease to exist. In (c) and in (d) we have plotted mean profiles for the SPDE and the frozen SPDAE systems. In each case we see a well defined front from the averaging and individual nucleations and annhilations are no longer distinguishable (although in (d) a large solution pollutes the data at $t \approx 130$ – this then ceased to exist at the next time step).

3.4. Computations using averaged quantities. Computing wave profiles using averaged quantities leads to the wave being 'polluted' by the spread of the individual waves (see [14]). We examine numerical solution of (2.10) where the time averaged wave speed $\Lambda(t)$ is used to fix the wave in the computational domain. However numerically this does not completely freeze each individual wave as we are now freezing with respect to an averaged quantity and the mean profile gives an indication of the position of the group of waves. We illustrate this in Figure 3.13 with results from a single realization in (a) which is not frozen (compare to Figure 3.1) and in (b) we plot the corresponding $\Lambda(t)$. In (c) the mean profile is plotted and shows a growth in the interval $[a(t), b(t)]$ and in (d) the corresponding $\Lambda(t)$ is plotted. One numerical advantage of computing a weaker quantity is that the computations are more stable as this reduces the variance in the convection term and there is less chance of switching from upwinding to downwinding and large convection terms.

4. Discussion. We have offered a generalized definition of a travelling wave that now depends on the choice of the reference function $\hat{u}$. This gives a defined quantity to consider which is particularly useful where a level set approach might fail such as for additive noise. This definition led to an efficient algorithm that allows the computation of stochastic travelling waves. We applied this to the Nagumo equation from mathematical biology however these computational techniques

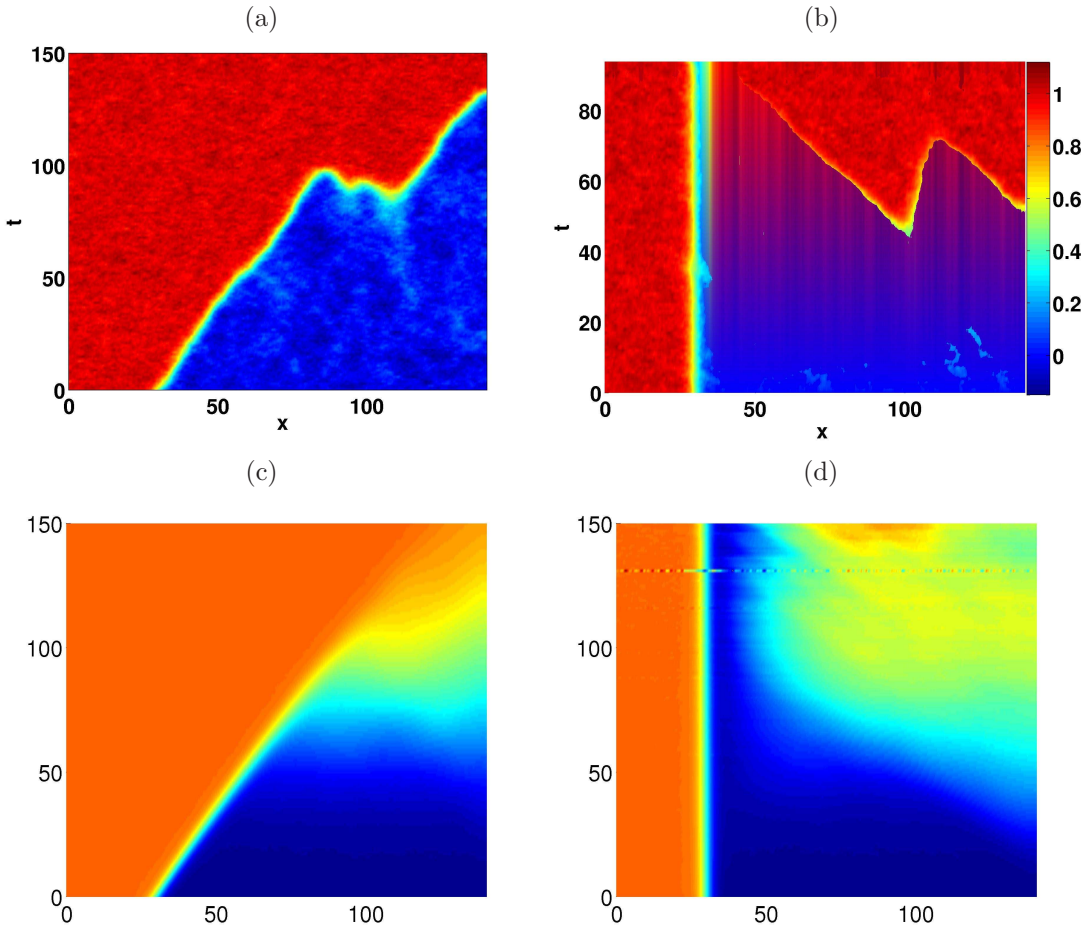

FIG. 3.12. *Nucleation of travelling waves and annihilation for the Nagumo equation with* $\alpha = 0.1$. *In (a) the space-time plot shows computations of the SPDE (no freezing) and in (b) the SPDAE where the wave is frozen. In (c) and (d) are plotted means over realizations for the frozen and travelling cases.*

can be applied to a host of other problems.

The algorithm described has several numerical advantages over simply solving the SPDE. When the wave travels and we solve the SPDE we need to take a large computational domain (we took $L = 650$ instead of $L = 60$) to ensure that the wave stays in the domain during the computation and is not affected by the boundary conditions. This has a number of consequences. To compute with the same spatial accuracy we obtain a much larger numerical system to solve. For this system we need to generate many more random numbers and so loose efficiency (this is particular true in this case where the wave has compact support). Furthermore we see in Figure 3.4 that at $t \approx 1800$ the travelling wave feels the boundary effects, which perturbs the convergence of the wave speeds, this is not evident just by examining the wave profile). Convergence is also slower for the SPDE and we used extrapolation to obtain the values of a, b and c. The accuracy of these quantities also seems less reliable, even for the deterministic case (see for example the remark towards the end of Section 3.1.1). The SPDAE approach avoids these difficulties.

A disadvantage of method is that by adding in the convection term leads numerical instabilities and to a fairly large number of solutions that fail to exist. We have seen in Section 3.1.2 and Section 3.1.3 that there is failure of the waves to exist when solved as the SPDAE which is not observed when simply solving the SPDE. This can be understood since we introduce large convection terms that that may change sign from one step to the next and introduce numerical instabilities. A more careful discretization of the convection term may improve this – for example

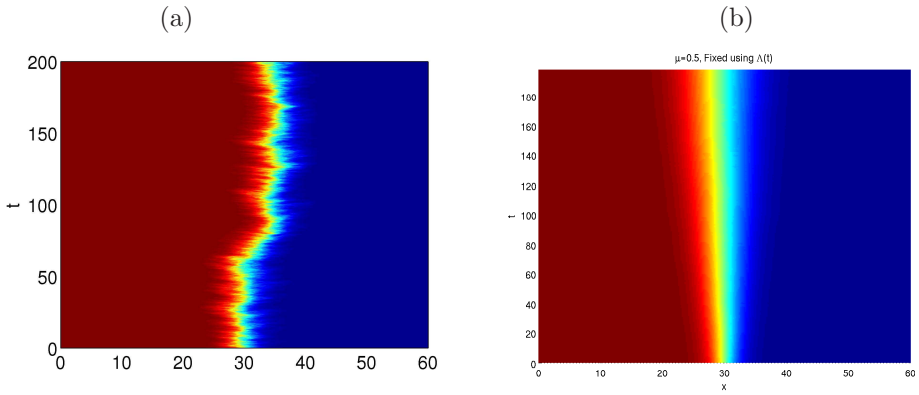

FIG. 3.13. *In (a) the solution from a single realization and in (b) the mean over* 1000 *samples. Here* (2.10) *was solved so the time-averaged wave speed* $\Lambda(t)$ *is used to 'fix' the wave for each realization and the mean profile spreads.*

predicting the sign of the instantaneous wave speed $\lambda(t)$ for (1.6) with $u^0 = u_{lin}$ and $\hat{u} = u_{det}$ can improve the number of solutions that exist to the final time by a factor of 10, but does not eliminate spurious extinctions. To avoid extinctions in the transients from initial data one possible practical solution is to solve with the wave travelling (computing λ) and to fix the wave after convergence of λ. Alternatively, if the domain size and computational demands are not an issue, then another option is not to fix the wave and simply to compute the instantaneous wave speeds $\lambda(t)$ and this approach is pursued in [10].

Our investigation of the Nagumo equation has revealed three interesting and new computational observations that we have not seen reported in the literature. For multiplicative Itô noise we see that spatial correlation seems to decrease the wave speed, as in Figure 3.8. Increasing the noise intensity does not always increase the wave speed, rather it depends on the nonlinearity, see Figure 3.9. For additive noise in the Nagumo equation we see that the wave speed is increased with the noise intensity like in the multiplicative case – this is probably because of the small perturbations ahead of the front make the wave faster.

There are a number of areas for further investigation, one of these is to investigate a stable implementation of the convection term. This would allow us with confidence to determine the extinction of solutions purely due to noise and eliminate those from numerically instability. It would also be interesting to examine existence through the minimization to a reference function as well as convergence of the method. Finally we note that such fixing techniques can also be applied to more general situations in the deterministic cases such as spiral waves [5, 6] and wave interactions [4] and these techniques should also apply to the stochastic case.

REFERENCES

[1] H. AIRAULT, *Équations asymptotiques pour des cas spéciaux de l'équation de Nagumo*, C. R. Acad. Sci. Paris Sér. I Math., 301 (1985), pp. 295–298.
[2] J. ARMERO, J. M. SANCHO, J. CASADEMUNT, A. M. LACASTA, L. RAMIIREZ-PISCINA, AND F. SAGUÉS, *External fluctuations in front propagation*, Phys. Rev. Lett., 76 (1996), pp. 3045–3048.
[3] U. M. ASCHER AND L. R. PETZOLD, *Computer methods for ordinary differential equations and differential-algebraic equations*, Society for Industrial and Applied Mathematics (SIAM), Philadelphia, PA, 1998.
[4] W.-J. BEYN, S. SELLE, AND V. THÜMMLER, *Freezing multipulses and multifronts*, Preprint 07-069, CRC 701, Bielefeld University, 2007.
[5] W.-J. BEYN AND V. THÜMMLER, *Freezing solutions of equivariant evolution equations*, SIAM Journal on Applied Dynamical Systems, 3 (2004), pp. 85–116.
[6] ———, *Numerical Continuation Methods for Dynamical Systems*, Series in Complexity, Springer, 2007, ch. Phase conditions, Symmetries, and PDE Continuation, pp. 301–330.
[7] S. BRASSESCO, A. DE MASI, AND E. PRESUTTI, *Brownian fluctuations of the interface in the* $d = 1$ *Ginzburg–Landau equation with noise.*, Annales de L'I.H.P. Section B., 31 (1995), pp. 81–118.
[8] Z. X. CHEN AND B. Y. GUO, *Analytic solutions of the Nagumo equation*, IMA J. Appl. Math., 48 (1992), pp. 107–115.

[9] P.-L. Chow, *Stochastic Partial Differential Equations*, Chapman & Hall, 2007.
[10] E. Coutts. PhD thesis, Heriot–Watt University, Inpreparation.
[11] G. Da Prato and J. Zabczyk, *Stochastic Equations in Infinite Dimensions*, vol. 44 of Encyclopedia of Mathematics and its Applications, Cambridge University Press, Cambridge, 1992.
[12] T. Funaki, *The scaling limit for a stochastic pde and the separation of phases*, Probability Theory and Related Fields, 102 (1995), pp. 221–288. DOI: 10.1007/BF01213390.
[13] J. García-Ojalvo, J. M. R. Parrondo, J. M. Sancho, and C. Van den Broeck, *Reentrant transition induced by multiplicative noise in the time-dependent ginzburg-landau model*, Phys. Rev. E, 54 (1996), pp. 6918–6921.
[14] J. Garcia-Ojalvo and J. M. Sancho, *Noise in Spatially Extended Systems*, Institute for nonlinear Science, Springer-Verlag, New York, 1999. ISBN 0-387-98855-6.
[15] S. A. J. Nagumo and S. Yoshizawa, *An active pulse transmission line simulating nerve axon.*, in Proceedings of the IRE, vol. 50, 1962, pp. 2061–2070.
[16] P. E. Kloeden and E. Platen, *Numerical solution of stochastic differential equations*, vol. 23 of Applications of mathematics, Springer–Verlag, 1992.
[17] G. J. Lord and J. Rougemont, *A numerical scheme for stochastic PDEs with Gevrey regularity*, IMA J Num. Anal., 24 (2004), pp. 587–604.
[18] A. S. Mikhailov, L. Schimansky-Geier, and W. Ebeling, *Stochastic motion of the propagating front in bistable media*, Physics Letters A, 96 (1983), pp. 453–456.
[19] C. Mueller and R. Sowers, *Travelling waves for the KPP equation with noise*, in Stochastic analysis (Ithaca, NY, 1993), vol. 57 of Proc. Sympos. Pure Math., Amer. Math. Soc., Providence, RI, 1995, pp. 603–609.
[20] D. Panja, *Effects of fluctuations on propagating fronts*, Physics Reports,, 393 (2004), pp. 87–174. doi:10.1016/j.physrep.2003.12.001.
[21] W. Römisch and R. Winkler, *Stochastic DAEs in circuit simulation*, in Modeling, simulation, and optimization of integrated circuits (Oberwolfach, 2001), vol. 146 of Internat. Ser. Numer. Math., Birkhäuser, Basel, 2003, pp. 303–318.
[22] J. Rougemont, *Space-time invariant measures, entropy, and dimension for stochastic Ginzburg-Landau equations*, Comm. Math. Phys., 225 (2002), pp. 423–448.
[23] C. W. Rowley, I. G. Kevrekidis, J. E. Marsden, and K. Lust, *Reduction and reconstruction for self-similar dynamical systems*, Nonlinearity, 16 (2003), pp. 1257–1275.
[24] O. Schein and G. Denk, *Numerical solution of stochastic differential-algebraic equations with applications to transient noise simulation of microelectronic circuit*, Journal of Computational and Applied Mathematics, 100 (1998), pp. 77–92.
[25] T. Shardlow, *Stochastic perturbations of the Allen–Cahn equation*, Electronic J. of Differential Equations, (2000), pp. 1–19. ISSN:1072-6691.
[26] T. Shardlow, *Numerical simulation of stochastic PDEs for excitable media*, J. Comput. Appl. Math., 175 (2005), pp. 429–446.
[27] T. Shiga, *Two contrasting properties of solutions for one-dimensional stochastic partial differential equations*, Canad. J. Math., 46 (1994), pp. 415–437.
[28] V. Thümmler, *Numerical Analysis of the method of freezing traveling waves*, PhD thesis, Bielefeld University, 2005.
[29] ———, *Asymptotic stability of discretized and frozen relative equilibria*, Preprint 06-030, CRC 701, Bielefeld University, 2006.
[30] R. Tribe, *A travelling wave solution to the Kolmogorov equation with noise*, Stochastics, 56 (1996), pp. 317–340.
[31] J. Walsh, *An introduction to stochastic partial differential equations.*, in Ecole d'ete de probabilites de Saint-Flour XIV, D. Williams, ed., vol. 1180 of Lect. Notes Math., Springer, 1986, pp. 265–437.
[32] R. Winkler, *Stochastic differential algebraic equations of index 1 and applications in circuit simulation*, J. Comput. Appl. Math., 157 (2003), pp. 477–505.
[33] ———, *Stochastic differential algebraic equations in transient noise analysis*, in Proceedings of 'Scientific Computing in Electrical Engineering', Mathematics in Industry, Sept 2004.